Nature & Technology

Modeling and simulation of the damage viscoplastic behavior of steel AISI 304

Zerouki Marzak* Ould Ouali Mohand, Khouas Aziz

Laboratoire Elaboration et caractérisation des matériaux et Modélisation, Université Mouloud MAMMERI de Tizi-Ouzou, BP 17 RP, 15000. ALGERIA.

Abstract

Understanding dynamic behavior of steel has gathered the efforts of many researchers during the last decades. Steel AISI 304 is the most widely used stainless steel. It has excellent forming and welding characteristics, extensively used in a variety of industries. Numerical modeling is often used in experimental investigations as full scale tests are expensive and may be impossible to conduct correctly. This is especially true for high and wide range of strain-rate events such as dynamic tensile.   In this work the damage viscoplastic behavior of steel AISI 304 will be microscopically modeled using the Abed-voyadjis model (physic model based on the thermal activation of dislocation) combined with the BONORA and BAI (lode angle criterion) damage criterion.   These models will be implemented in Abaqus / Explicit, we used the VUMAT (Vector zed User MATeriel) user subroutine and radial return mapping algorithm to solve incremental problems. Finally, we realize numerical simulations in Abaqus/Explicit for different rate strain on the tensile specimens (flat), and we compare numerical results obtained by our model with the experimental results.

Key words: AISI 304, viscoplastic, damage, Abed-voyadjis model, Bonora model, Bai model, Lode angle, dynamic tensile, Abaqus/Explicit, Vumat.

1.Introduction

Modern engineering technologies have placed increasing demands for constitutive modeling and the knowledge of material parameters at high strain rates, for this reason many computer codes exist which can be used to perform computations of complex structures under dynamic loading conditions like intense impulsive loading due to high-velocity impact(for example: Abaqus). The main requirement of large deformation problems such as life prediction; impact, and metal forming, is to develop constitutive relations which are widely applicable and capable of accounting for complex paths of deformation. Steel AISIS 304 are the most versatile and widely used of all the stainless steels. Their chemical composition,

mechanical properties, weld ability and corrosion/oxidation resistance provides the best all-round performance at relatively lower cost.

In this paper the damage viscoplastic behavior of steel AISI 304 will be microscopically modeled using the Abed-voyadjis model, based on the thermal activation of dislocation, combined with damage criterion: the BONORA model and BAI model (based on the lode angle criterion). These models will be implemented in Abaqus / Explicit [1], we used the VUMAT (Vector zed User MATeriel) user subroutine [2] and radial return mapping algorithm [3] to solve incremental problems. Finally, we realize numerical simulations in Abaqus/Explicit for different rate strain on the tensile specimens (flat), and we compare numerical results obtained by our model with the experimental results.

2.Modélisation numérique
2.1. Abed-Voyadjis model

The Abed-Voyadjis model was proposed by Abed and Voyadjis [4-6] based on the thermal activation theory of dislocations. Elias Farah [7] proposed a model inspired micromechanical mechanisms but defined by phenomenological parameters identified from the behavior macroscopique.la flow stress is given by the following expression:

$$\sigma = \sigma_e + K\left(\overline{\varepsilon}^p\right)^{\frac{1}{M}}\left\{1-\left[A\left(\overline{\varepsilon}^p\right)^{\frac{1}{2}}T - BT\,ln\left(\frac{\dot{\overline{\varepsilon}}^p}{\dot{\overline{\varepsilon}}_0^p}\right)\right]^{\frac{1}{q_1}}\right\}^{\frac{1}{q_2}}$$

(1)

with *A*, *B*, *K*, *M*, q_1 and q_2 represent material parameters.

$\dot{\overline{\varepsilon}}_0^p$: **The reference plastic strain rate is usually taken equal 10^{-6} s^{-1} [8];**

$\overline{\varepsilon}^p$: **The equivalent plastic strain.**

$$\overline{\varepsilon}^p = \int_0^t \sqrt{\left(\frac{2}{3}\dot{\varepsilon}^p : \dot{\varepsilon}^p\right)}\,dt$$

(2)

With $\dot{\varepsilon}^p$ is the tensor of the plastic deformation rate and t is the time.

$\dot{\overline{\varepsilon}}^p$: **Equivalent plastic strain rate.**

$$\dot{\overline{\varepsilon}}^p = \sqrt{\frac{2}{3}\dot{\varepsilon}^p : \dot{\varepsilon}^p}$$

(3)

σ_e : **The yield stress of the material.**

2.2. Damage criterion

The law of damage evolution is an integral part of a report by linear increase is assumed between the indicator D damage and stress equivalent plastic.

$$D = \frac{\overline{\varepsilon}^p}{\varepsilon_f}$$

(4)

Bonora and al. [9-10] gives the damage variable by the following expression:

$$\dot{D} = \alpha\frac{(D_{cr} - D_0)^{\frac{1}{\alpha}}}{ln\left(\frac{\varepsilon_f}{\varepsilon_d}\right)}f(\eta)(D_{cr} - D)^{\frac{\alpha-1}{\alpha}}\frac{\dot{\overline{\varepsilon}}^p}{\overline{\varepsilon}^p}$$

(5)

With D_{cr} is the critical value of damage beyond which there is rupture, D_0 is the initial damage, α is a material parameter, ε_f is plastic deformation of rupture, ε_d is plastic deformation below which the damage remains zero. The effect of stress triaxiality is given by the function f (η)

$$f(\eta) = \frac{2}{3}(1+\nu) + 3(1-2\nu)(\eta)^2$$

(6)

where ν is the Poisson coefficient of the material.

The plastic strain at rupture is considered as constant, which can be represented a limitation to this model. That is why we used the strain at rupture proposed by Bai and al. [11]

$$\varepsilon_f\left(\eta,\overline{\theta}\right) = \left[\frac{1}{2}\left(D_1 e^{-D_2\eta} + D_5 e^{-D_6\eta}\right) - D_3 e^{-D_4\eta}\right]\overline{\theta}^2$$
$$+\frac{1}{2}\left(D_1 e^{-D_2\eta} + D_5 e^{-D_6\eta}\right)\overline{\theta} + D_3 e^{-D_4\eta}$$

(7)

with *η* the triaxialité expressed by:

$$\eta = \frac{\sigma_m}{\overline{\sigma}}$$ (8)

θ: is lode angle given between 0 and $\frac{\pi}{3}$ ($0 \leq \theta \leq \frac{\pi}{3}$)

ζ: is normalized third deviatoric stress invariant, $-1 \leq \xi \leq 1$.[12-13]

$$\xi = cos(3\theta)$$ (9)

$\overline{\theta}$: is the lode angle equivalent give through

$$\overline{\theta} = 1 - \frac{2}{\pi} ar cos(\xi)$$ (10)

So the equation becomes:

$$D = \frac{\overline{\varepsilon}}{\varepsilon(\eta, \overline{\theta})}$$ (11)

3.Implementation

The model described above was implemented in the Abaqus/explicit using user subroutine VUMAT (Vectorized user materiel) and exploiting the radial Return Mapping Algorithm. The yield function denoted **f** given by

$$f(\sigma, p, \dot{p}, T) = \sigma^{eq} - \sigma$$ (12)

Where σ^{eq} represent the von Mises stress .For any stress we have three possible cases:

• **If** $f(\sigma, p, \dot{p}, T) \prec 0$ **elastic;**

• **If** $f(\sigma, p, \dot{p}, T) = 0$ **et** $\dot{f} = 0$ **inelastic load. The plastic multiplier is calculated from the consistency conditions** $\dot{f} = 0$ **.**

•**If** $f(\sigma, p, \dot{p}, T) = 0$ **and** $\dot{f} \prec 0$ **unloading.**

For each increment of time Δt and strain $\Delta \varepsilon$ known, we assume that the initial variable states are known. The steps followed during implementation are:

• **After strain increment** $\Delta \varepsilon$ **, if the value of the damage variable D exceeds a critical value $D_{cr}= 1$ we have:**

$$\sigma_{n+1} = 0$$ (13)

The other state variables do not change:

$$\varepsilon_{n+1}^p = \varepsilon_n^p$$ (14)

$$\overline{\varepsilon}_{n+1}^p = \overline{\varepsilon}_n^p$$ (15)

$$T_{n+1} = T_n$$ (16)

$$R_{n+1} = R_n$$ (17)

$$\lambda_{n+1} = \lambda_n$$ (18)

$$D_{n+1} = D_n$$ (19)

The indices *n* and *n* + 1 are related to the beginning and the end of the increment respectively. Else we go to the next step: the elastic prediction and calculates the stress trial.

• **In this step we assume that the strain increment is elastic:**

$$\Delta \varepsilon = \Delta \varepsilon^e$$ (20)

The stress trial is expressed by:

$$\sigma_{n+1}^* = \sigma_n + (1-D)E : \Delta \varepsilon$$ (21)

E is the tensor of elastic module. This stress is evaluated elastically. We will check in the next step that is still in the elastic loading.

• **Calculation of the yield function for the value of the stress trial** σ_{n+1}^* **:**

$$f = \sigma_n^{eq*} - \sigma \tag{22}$$

With σ^{eq*} is the equivalent stress of Von Mises calculated from the stress trial.

$$\sigma^{eq*} = \sqrt{\frac{3}{2}\sigma_{n+1}^* : \sigma_{n+1}^*} \tag{23}$$

• if $f \leq 0$ the material will always remain in the elastic loading, so the value of the stress trial σ_{n+1}^* is acceptable.

$$\sigma_{n+1} = \sigma_{n+1}^* \tag{24}$$

The state variables remain unchangeable:

$$\varepsilon_{n+1}^p = \varepsilon_n^p \tag{25}$$

$$\overline{\varepsilon}_{n+1}^p = \overline{\varepsilon}_n^p \tag{26}$$

$$T_{n+1} = T_n \tag{27}$$

$$R_{n+1} = R_n \tag{28}$$

$$\lambda_{n+1} = \lambda_n \tag{29}$$

with

ε^p : The tensor plastic strain;

λ : The plastic multiplier;

R : The isotropic hardening;

T : Temperature.

We will return to step 1 for next increment.

• If $f > 0$ the material undergoes a viscoplastic strain, the stress trial should be corrected.

$$\sigma_{n+1} = \sigma_{n+1}^* - 2\mu N_{n+1}\Delta\lambda \tag{30}$$

With μ is Lamé coefficient.

$$\mu = \frac{E}{2(1+\nu)} \tag{31}$$

The hypothesis of the plastic incompressibility and isotropic hardening requires the evolution of the stress is radial and tensors normal to the surface are equal.

$$N_{n+1} = N_{n+1}^* = \frac{3}{2}\frac{\sigma_{n+1}^*}{\sigma_{n+1}^{eq*}} \tag{32}$$

The equation of the normal N of the load surface is readily assessed since the only unknown in the relationship (30) is the increment of plastic multiplier $\Delta\lambda$.

Other constitutive equations are also in terms of $\Delta\lambda$.

$$\sigma_{n+1}^{eq} = \sigma_{n+1}^{eq*} - 2\mu\Delta\lambda \tag{33}$$

$$\varepsilon_{n+1}^p = \varepsilon_n^p + N_{n+1}\Delta\lambda \tag{34}$$

$$\overline{\varepsilon}_{n+1}^p = \overline{\varepsilon}_n^p + \Delta\lambda \tag{35}$$

$$T_{n+1} = T_n + \Delta T \tag{36}$$

$$R_{n+1} = R_n + \Delta R \tag{37}$$

$$D_{n+1} = D_n + \Delta D \tag{38}$$

where

$$\Delta T = \frac{1}{\rho c_p} \left(\sigma_{n+1}^{eq} - R_{n+1} \right) \Delta\lambda \tag{39}$$

$$\Delta R = \frac{K}{M} \chi_{n+1} \left(\overline{\varepsilon}_{n+1}^{p} \right)^{(1-M)/M} \Delta\lambda \tag{40}$$

$$\Delta D = \alpha \frac{\left(D_{cr} - D_0 \right)^{\frac{1}{\alpha}}}{ln\left(\frac{\varepsilon_f}{\varepsilon_d} \right)} f\left(\sigma^* \right) \left(D_{cr} - D_n \right)^{\frac{\alpha-1}{\alpha}} \frac{\dot{\overline{\varepsilon}}_{n+1}^{p}}{\overline{\varepsilon}_{n+1}^{p}} \tag{41}$$

$$\chi_{n+1} = \left\{ 1 - \left[A\left(\overline{\varepsilon}_{n+1}^{p} \right)^{\frac{1}{2}} T_{n+1} - B T_{n+1} ln\left(\frac{\Delta\lambda}{\dot{\overline{\varepsilon}}_0 \Delta t} \right) \right]^{\frac{1}{q_1}} \right\}^{\frac{1}{q_2}} \tag{42}$$

- **The relations (33) to (38) are replaced in yield function** *f*.

$$f(\Delta\lambda) = \sigma_{n+1}^{eq*} - 3\mu\Delta\lambda - \sigma \tag{43}$$

Such as

$$\sigma = \sigma_e + K\left(\overline{\varepsilon}_{n+1}^{p} \right)^{\frac{1}{M}} \left\{ 1 - \left[A\left(\overline{\varepsilon}_{n+1}^{p} \right)^{\frac{1}{2}} T_{n+1} - B T_{n+1} ln\left(\frac{\Delta\lambda}{\dot{\overline{\varepsilon}}_0 \Delta t} \right) \right]^{\frac{1}{q_1}} \right\}^{\frac{1}{q_2}} \tag{44}$$

- **This step is to solve the equation (26) by the method of Newton-Raphson.**

$$\Delta\lambda^{i+1} = \Delta\lambda^{i} - \frac{f\left(\Delta\lambda^{i} \right)}{f^{'}\left(\Delta\lambda^{i} \right)} \tag{45}$$

where

$$f^{'}\left(\Delta\lambda^{i} \right) = -3\mu + \frac{\partial f}{\partial p} \frac{\partial p}{\partial \Delta\lambda} + \frac{\partial f}{\partial T} \frac{\partial T}{\partial \Delta\lambda} + \frac{\partial f}{\partial \dot{p}} \frac{\partial \dot{p}}{\partial \Delta\lambda} \tag{46}$$

- **Once the value of** $\Delta\lambda$ **is determined, the state variables are known. For a new increment of strain** $\Delta\varepsilon$ **and time** Δt **, the resulting state variables are considered initials and we return to the first step in identifying the new values of the state variables at the end of each increment.**

4. Simulation numeric

4.1 Material studied and specimen

Steel AISI 304 is the most widely used stainless steel. It has excellent forming and welding characteristics: High ductility, excellent drawing, forming, and spinning properties. Essentially non-magnetic, becomes slightly magnetic when cold worked. Low carbon content means less carbide precipitation in the heat-affected zone during welding and a lower susceptibility to intergranular corrosion . Extensively used in a variety of industries, its typical applications include: pipelines, heat exchanger railings, springs or threaded fasteners marine equipment and fasteners, nuclear vessels, refrigeration equipment, paper industry, pressure vessels and valves.

These experimental studies were carried out by Rusinek and al. [14].The tables below represent Chemical composition and Physical constants of steel AISI 304.

Table 1. Chemical composition of steel AISI 304 [15]

C	Mn	Cr	Ni	Mo	Cu	Si	Nb
0.06	1.54	18.47	8.3	0.30	0.37	0.48	0.027

Table 2. Physical constants for steel AISI 304. [15]

E(GPa)	$C_p(JKgK^{-1})$	υ	$\rho(Kgm^{-3})$
200	470	0.3	7800

In figure below shows the geometry and dimensions of the tensile specimen.
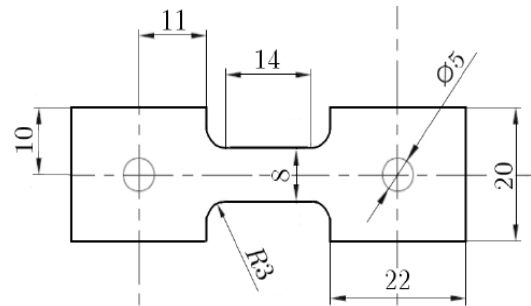
Figure 1. Geometry and dimensions of the tensile specimens in *mm*.[16]

4.2 Description of the conditions of the simulation

Consider volume element (1x1x1),We imposed a longitudinal locking movement of the nodes in the axis Y, and a strain rate imposed on the axis X to the nodes of the specimen.
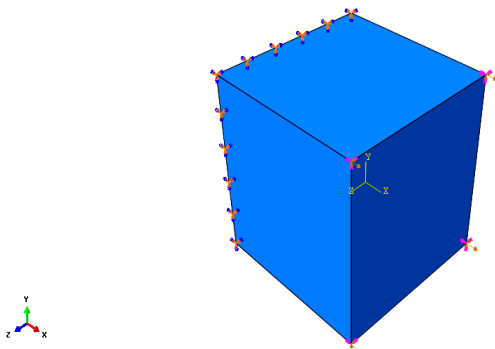
Figure 2. Boundary conditions and loading used in the simulation.

4.3 Result and discussion

In this section we apply the model described above in order to simulate the behavior of a specimen under tensile loading at different strain rate ($\dot{\varepsilon}$ =0.01 s^{-1} and $\dot{\varepsilon}$ =0.02 s^{-1}).

The tables 3, 4 and 5 represent the material constants of the models abed-Voyadjis, Bonora and Bai respectively.

Table 3. Material constants of the Abed-Voyadjis model for steel AISI 304.

A (K^{-1})	B (K^{-1})	K (MPa)	M	q$_1$	q$_2$	ε_{i0} (s^{-1})
0.000049	0.00156	2100	1.3	0.5	1.5	10^{-6}

Table 4. Material constants of the Bonora damage model for steel AISI 304

D$_c$	α	ε_d
1	0.2	0.0016

Table 5. Material constants of Bai and al. damage model for steel AISI 304.

D$_1$	D$_2$	D$_3$	D$_4$	D$_5$	D$_6$	θ
0.3	-1.4	0.2	-0.6	0.23	-0.4	0.8

Figures 3 and 4 illustrate respectively the deformation of specimen and stress/strain curve for numerical and experimental results at strain rate $\dot{\varepsilon}$ = 0.01 s^{-1} and temperature T=298K.
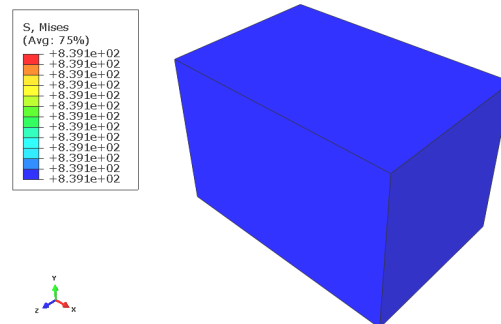
Figure 3. Deformation of volume element for strain rate $\dot{\varepsilon}$ = 0.01 s^{-1} and temperature T =298K.
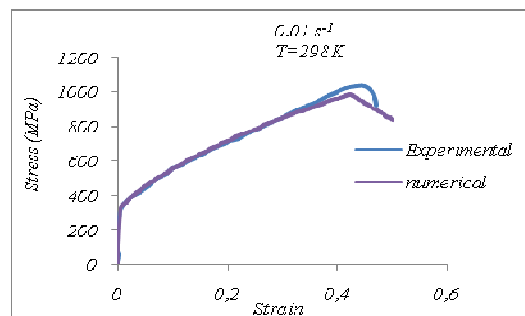
Figure 4. Stress/strain Curve for numerical and experimental results at strain rate $\dot{\varepsilon}$ = 0.01 s^{-1} and temperature T=298K.

Figures 5 and 6 present respectively the deformation of specimen and stress/strain curve for numerical and experimental results at strain rate $\dot{\varepsilon}$ = 0.002 s^{-1} and temperature T=293K.
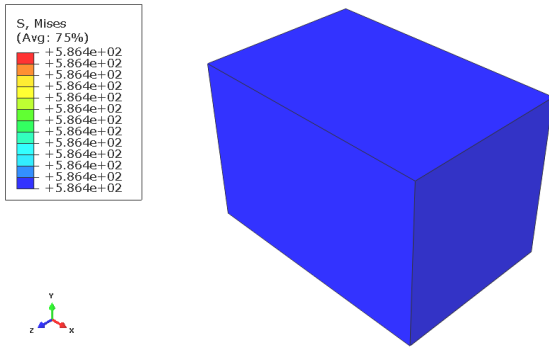
Figure 5. Deformation of volume element for strain rate

$\dot{\varepsilon}$ = 0.01 s^{-1} and temperature T =293K.

$\dot{\varepsilon}$ = 0.002 s^{-1} and T=293K
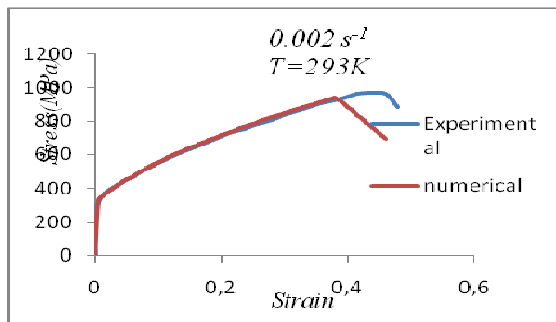
Figure 6. Stress/strain Curve numerical and experimental for strain rate $\dot{\varepsilon}$ = 0.002 s^{-1} **and temperature T=293K.**

Figure 4 and 6 evoke the comparison between the results numerical obtained by Abed-Voyadjis combined with Bonora and Bai damage, and the experimental results for strain rate ($\dot{\varepsilon}$ =10^{-2}s^{-1} and $\dot{\varepsilon}$ =2.10^{-3}s^{-1}). According to these comparisons, One notices that the increase strain rate generates an increase in the stress. The numerical models correctly describe the viscoplastic damage behavior of steel AISI 304, for the good superposition between the numerical and experimental curves.

5. Conclusion

In this paper, we were interested the modeling of the damage viscoplastic behavior of steel AISI 304 with a approach physical Abed-Voyadjis combined with Bonora and Bai damage model. These models predicted successfully the behavior of the steel AISI 304 studied during the dynamic tensile test ($\dot{\varepsilon}$ =0.01s^{-1} and $\dot{\varepsilon}$ =0.002s^{-1}), for good coherence between the numerical and experimental results.

In prospects, we envisage an extension of this model to take into account kinematic hardening and anisotropy, this for a more precise and complete modeling.

References

[1]   Ould Ouali, M.; Aberkane, M. Micromechanical modeling of the roling of a A1050P aluminum sheet. International Journal of Material Forming 2009, vol.2, Issue.1,pp. 25-36.

[2]   Larbi, S. ; Ould Ouali, M.; Bennabes, A. Comparison of explicit and implicit finite element simulations of void growth and coalescence in porous ductile materials. Materials and Design. 2008, vol 29(2), pp. 319-329.

[3]   Qidwai, M. A.; Lagoudas, D.C. Numerical implementation of a shape memory alloy thermomechanical constitutive model using return mapping algorithms. Int. J. Numer. Meth. Engng .2000, 47,1123-1168.

[4]   Voyiadjis, G.; Abed, F. Effects of dislocation density evolution on the thermomechanical response of metals with different crystal structures at low and high strain rates and temperature. Archives of Mechanics.2005a, 57(4), 299 – 343.

[5]   Voyiadjis, G.; Abed, F. Microstructural based models for bcc and fcc metals with temperature and strain rate dependency. Mechanics of Materials. 2005b, 37, 355 – 378.

[6]   Voyiadjis, G.; Abed,F. Implicit algorithm for finite deformation hypoelastic-viscoplasticity in fcc metals. International Journal for Numerical Methods in Engineering 2006b, 67, 933 – 959.

[7] **Farah, E. Modèle constitutif du comportement viscoplastique d'un Matériau CFC. Maîtrise des sciences appliquées. Thesis, département génie mécanique, Ecole polytechnique de Montréal, University of Montréal, 2009.**

[8] **Kocks, U.; Mecking, H. Physics and phenomenology of strain hardening: the FCC case. Progress in Material Science 2003, 48,171 – 273.**

[9] **Bonora, N.; Gentile, D.; Pirondi, A.; Newaz, G. Ductile damage evolution under triaxial state of stress: theory and experiments. International Journal of Plasticity. 2005, 21, 981–1007.**

[10] **Bonora, N.; Ruggiero, A. Micromechanical modeling of ductile cast iron incorporating damage. Part i : Ferritic ductile cast iron. International journal of solids and structures .2005, 42, 1401–1424.**

[11] **Bai, Y.; Wierzbicki, T. A new model of metal plasticity and fracture with pressure and lode dependence. International Journal of Plasticity. 2008,24,071-1096.**

[12] **Malvern, L.E.. Introduction to the Mechanics of a Continuous Medium. Prentice-Hall, Inc. 1969.**

[13] **Xu, B.; Liu, X. Applied Mechanics: Elasticity and Plasticity. Tsinghua University Press, 1995, Beijing, China.**

[14] **Rusinek and al. Experimental characterisation and modeling of the thermo-viscoplastic behaviour of steel aisi 304 within wide ranges of strain rate at room temperature. Journal of theoretical and applied mechanics. 2010, 48, 4, pp. 1027-1042.**

[15] **De and al. Deformation-induced phase transformation and strain hardening in type 304 austenitic stainless steel. *Metall. and Mat. Trans* . 2006, A37, 1875-1886.()**

[16] **Rusinek, A.; Cheriguene, R.; Baumer, A.; Larour, P.Dynamic behavior of high-strength sheet steel in dynamic tension: experimental and numerical analyses. J. of Strain Analysis for Engineering 2008, 43, 37-53.**